

Estimation of ductility of RC members under load reversals

Nibaldo B. Avilés
 University of La Serena, Chile

Kyuichi Maruyama
 Nagaoka University of Technology, Japan

ABSTRACT: In order to estimate the ductility of reinforced concrete (RC) members with various reinforcement, such as transverse reinforcement (hoops), steel plate wrapping, and combination of them, the stress strain behavior of confined concrete with above reinforcement was, first, examined under uniaxial compression. The contribution of various reinforcement was quantitatively evaluated, and the estimation method of the ductility of RC members was proposed.

1 INTRODUCTION

The ductility of reinforced concrete members is highly influenced by the behavior of confined concrete. In order to expand the understandings on the behavior of confined concrete, a lot of experimental study have been done and many analytical models have been developed. However, the most effort has concentrated on the use of spirals or ties as transverse reinforcement, such as Scott et al. (1982), Park et al. (1982), Shah et al. (1983), etc.

On the other hand, strengthening the RC members by steel plate wrapping has been applied to the existing structures, and was reported effective to improve the ductility of members. The mechanism of how the steel plate wrapping contributes to the ductility improvement is not clear, and the quantitative evaluation method is not yet established.

As far as the basic function is concerned, both the transverse reinforcement and the steel plate play the same role as confinement of concrete. The difference lies only in how effectively they work. It should be, then, possible to treat them in the same manner by developing a proper model to evaluate their effects on the confinement of concrete.

It is mainly discussed in this paper how the transverse reinforcement (hoops), the wrapped steel plate and their combination influence the stress-strain behavior of concrete under the uniaxial compression load. A particular attention was paid to the deformation behavior after the maximum load. Considering the strain localization the ductility improvement measures were evaluated in terms of the stress-strain behavior

of concrete in the fracture process zone.

Based on the proposed quantitative evaluation method for the contribution of various reinforcement on the strain localization and stress strain behavior of concrete, the ductility of RC columns under load reversal was examined.

2 STRESS STRAIN BEHAVIOR OF CONFINED CONCRETE

In the experimental program specimens were tested under uniaxial compression load, having the parameters such as the cross section shape, the type and amount of transverse reinforcement. The cross section was circular and rectangular. The transverse reinforcement consisted of hoops, steel plate wrapping, anchor bolts on the plate, and combinations of above. The spacing of hoops were 2.5, 5 and 10 cm.

To ensure the effectiveness of hoops four $\phi 10$ mm bars were used in the longitudinal direction. The steel grade was SD-30 (294 N/mm²) for steel bars, G3101-SS30 (294 N/mm²) for steel plate. The anchor bolts were commercial bolts of $\phi 6$ mm with embedment length of 50 mm. The steel plate thickness was 1.2 mm. The design strength of

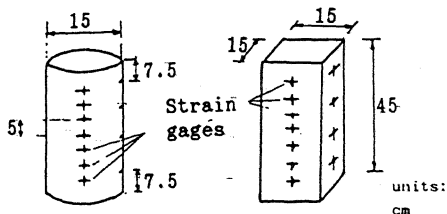


Fig.1 Test specimens

Table 1. Test Specimens

Cylinders	Prisms	Reinforcement
C-S0	P-S0	Plain concrete
C-S0-P	P-S0-P	Steel plate
C-S10-P	P-S10-P	Hoops and steel plate
C-S10	P-S10	Hoops $\phi 6 @ 10$ cm
C-S5	P-S5	Hoops $\phi 6 @ 5$ cm
C-S2.5	P-S2.5	Hoops $\phi 6 @ 2.5$ cm
C-S0-PS	P-S0-PS	Steel plate strips (5 cm width)
C-S0-P-B	P-S0-P-B	Steel plate and anchor bolts
C-S10-P-B	P-S10-P-B	Hoops, steel plate and anchor bolts

concrete ($\phi 10 \times 20$ cm cylinders) was 37.5 N/mm^2 .

The deformation of specimen was measured by two dial gages for overall deflection and by strain gages which were attached to the specimen at 5 cm intervals in the longitudinal direction.

The dimensions of specimen and the location of strain gages are shown in Fig. 1, and the details of specimens are indicated in Table 1.

The load was applied monotonically by an actuator of 1960 kN capacity and it was controlled at first by loading rate and then by deformation rate after reaching to 80% of the maximum load of the specimen. In order to reduce the excentricity, the definitive loading was applied only when the difference of strain measurements in the

four sides became less than 10%.

2.1 Load-displacement relationships

Fig. 2 shows the load-displacement relationships of cylinder and prism specimens. As being expected, the specimens with steel plate reinforcement presented considerably large ductility than those with hoops. The specimen with hoops at 2.5 cm spacing (C-S2.5 and P-S2.5) presented good ductility, but not large enough to compare with the cases of the steel plate strips (C-S0-PS and P-S0-PS), where the role of steel plate was remarkable for prevention against the drastic reduction of capacity at large deflection levels. The steel plate strips showed an intermediate effect between the specimen with hoops at 2.5 cm spacing and the specimen with steel plate only. It was also observed that the presence of steel plate made the displacement at the maximum load increase.

In general, the presence of bolts contributed to increase the displacement rather than the load in the post peak range.

By comparing Figs. 2(a) and 2(b) it was evident that the effectiveness of reinforcement was greater for the circular cross section than for the rectangular section, as was expected.

2.2 Strain localization

Examination of strain measurements in the longitudinal direction showed the strain localization after passing the maximum strength. As shown in Fig. 3, the strain distribution was almost uniform up to the peak load (P_0), but in the strain softening range after peak load the fracture process zone formed with a certain width (w) and the strain began to localize in the zone.

In order to obtain the stress-strain relationship in the fracture process zone, the load displacement relationships were transformed by setting the compatibility

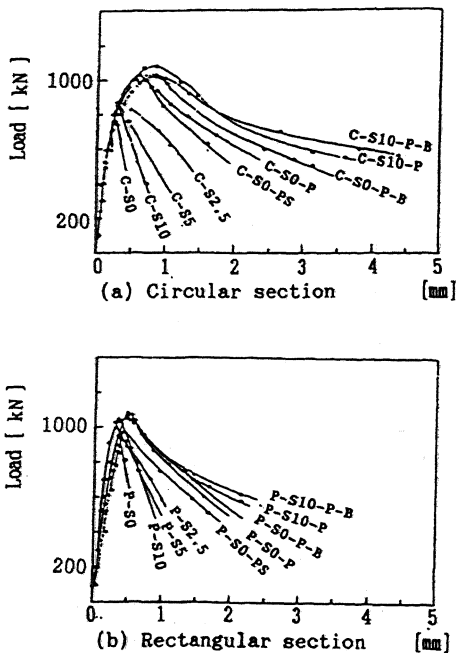


Fig. 2 Load-displacement relationships

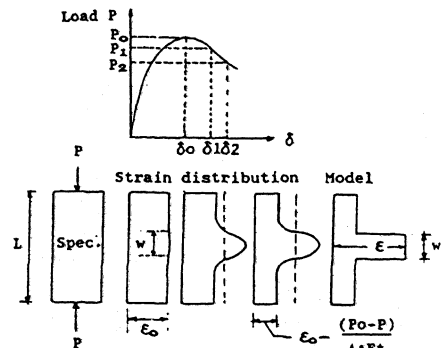


Fig. 3 Strain distribution model

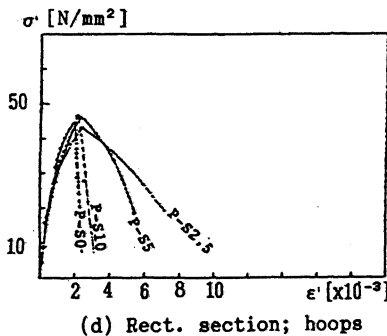
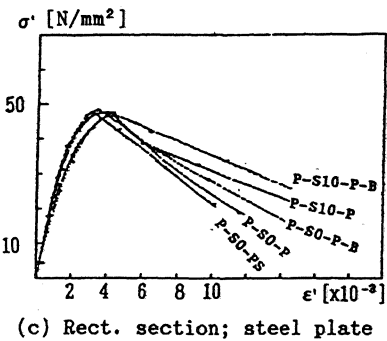
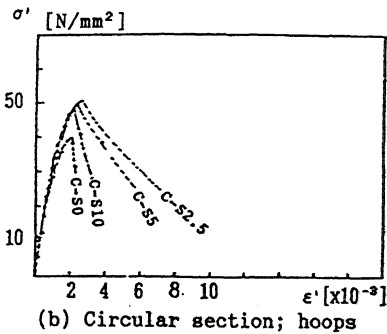
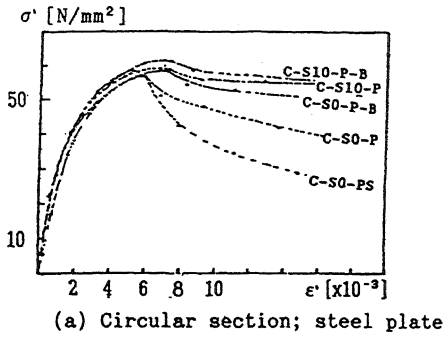


Fig. 4 Stress-strain relationships

equation, which was based on the modeled strain distribution in Fig. 3 and given by Eq. (1)

$$(\epsilon - \epsilon_o) \cdot w = (\delta - \delta_o) + \frac{(P_o - P)}{A \cdot E_t} \cdot (L - w) \quad (1)$$

where ϵ_p = mean plastic strain in the fracture process zone; w = width of the fracture process zone; δ = overall displacement of specimen; P = applied Load; L = specimen length; E_t = tangent modulus of concrete; and A = cross sectional area of specimen. The stress-strain curves obtained for each specimen are shown in Fig. 4.

2.3 Stress-strain characteristics in fracture process zone

For quantitative evaluation of the effect of reinforcement, it is necessary to express the effect in the explicit formulas. Therefore, the effect of reinforcement was, hence, examined as to the stress-strain characteristics in the fracture process zone.

The analytical equation for the stress-strain can be taken as follows: for the ascending part

$$\sigma' = f'_{oc} \cdot [1 - \frac{\epsilon'}{\epsilon'_{oc}}]^2 \quad (2)$$

and for the descending part

$$\sigma' = f'_{oc} \cdot \exp[-k(\epsilon' - \epsilon'_{oc})] \quad (3)$$

where, f'_{oc} = maximum strength of confined concrete; ϵ'_{oc} = strain at the maximum strength; and k = a constant to define the descending part.

To represent the confinement condition of the concrete, a confinement index α was introduced as

$$\alpha = \rho_{sh} \frac{f_{yh}}{f'_c} \lambda_{1h} \lambda_{2h} + \rho_{sp} \frac{f_{yp}}{f'_c} \lambda_{2p} \quad (4)$$

where, ρ_{sh} , ρ_{sp} = ratios of total volume of transverse reinforcement to volume of concrete core, hoop and steel plate respectively; f_{yh} , f_{yp} = the yield strengths of hoop and steel plate respectively; f'_c = the concrete strength; λ_1 = a factor to consider the hoop spacing effect, and λ_{2h} , λ_{2p} = factors to consider the effectiveness of confinement for rectangular sections with hoops and steel plate respectively.

For circular and square sections with steel plate wrapping,

$$\rho_{sp} = \frac{t \cdot (d-t) \cdot L_{plate}}{0.25 \cdot (d-2t) \cdot L} \quad (5)$$

in which t = steel plate thickness; d = diameter or width of specimen; L_{plate} = length of plate or the effective total length of strips; and L = length of specimen.

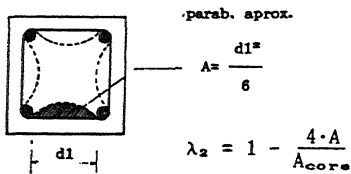


Fig. 5 λ_2 calculation

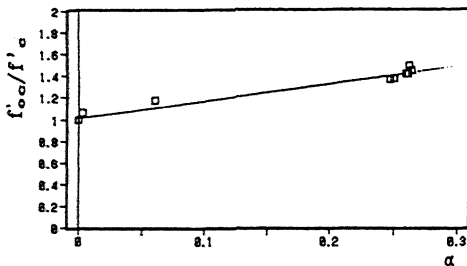


Fig. 6 $f'_{oc}/f'_c - \alpha$ relation

If the spacing (s) exceeds the value of about 1.25 times the minimum dimension of concrete core d_c , the effects of confinements become negligible as Shah et al. (1983) indicated, then

$$\lambda_1 = 1 - \frac{s}{1.25d_c} \quad (6)$$

Fig. 5 indicates how to calculate λ_2 value based on Sheikh et al. (1982). Fig. 6 shows the influence of confinement index α on the compressive strength of confined concrete using the regression analysis, the linear function was found as Eq.(7). Similar relationships were obtained for $f'_{oc}/f'_c - \epsilon_{oc}/\epsilon_o$, $f'_{oc}/f'_c - k/k_o$ and $f'_{oc}/f'_c - k/k_o$. The empirical derived equations are as follows

Circular section:

$$f'_{oc} = (1 + 1.681\alpha)f'_c \quad (7)$$

$$\epsilon'_{oc} = (-3.447 + 4.447f'_{oc}/f'_c)\epsilon'_o \quad (8)$$

$$k = \exp(-8.1027(f'_{oc}/f'_c - 1))k_o \quad (9)$$

$$w = (-1.040 + 1.140f'_{oc}/f'_c)L \quad (10)$$

$$\epsilon'_o = 2040 \times 10^{-6} \quad (11)$$

$$k_o = 0.001007 \quad (12)$$

Rectangular section:

$$f'_{oc} = (1 + 1.352\alpha)f'_c \quad (13)$$

$$\epsilon'_{oc} = (-2.283 + 3.283f'_{oc}/f'_c)\epsilon'_o \quad (14)$$

$$k = \exp(-13.3317(f'_{oc}/f'_c - 1))k_o \quad (15)$$

$$w = (-1.535 + 1.635f'_{oc}/f'_c)L \quad (16)$$

$$\epsilon'_o = 2010 \times 10^{-6} \quad (17)$$

$$k_o = 0.002971 \quad (18)$$

Fig. 7 indicates the comparison of stress-strain curves obtained from tests and from formulas proposed in this paper.

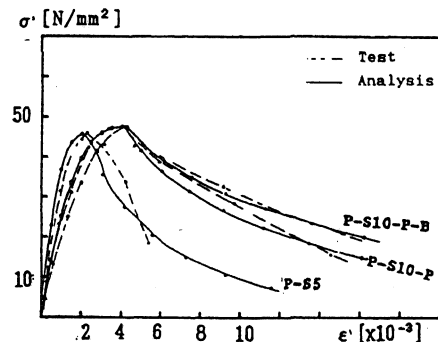
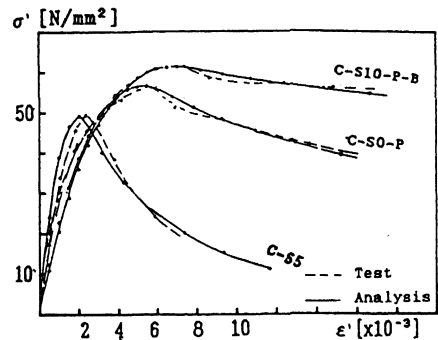


Fig. 7 Comparison between test and analytical stress-strain curves

3 DUCTILITY BEHAVIOR OF RC COLUMNS

In the experimental program, four columns specimens were tested under incrementally increased load reversals. The parameters were the type and the amount of the transverse reinforcement in the critical zone between the fixed end and a distance of 1.5 times the effective depth. The sectional properties of the columns were almost identical to each other, but the arrangement of transverse reinforcement was designed in four different types, such as (1) having no hoop (2) with hoops (3) steel plate wrapping only and (4) with hoops and steel plate wrapping (Fig. 8).

The transverse reinforcement consisted of hoops of $\phi 6$ mm with 10 cm spacing, and of steel plate with 1.3 mm thickness. Longitudinal reinforcement was the same in all the specimens and consisted of $4\phi 19$ mm.

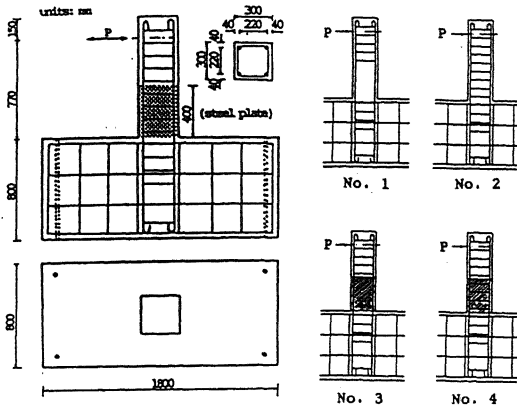


Fig. 8 Test specimens

The design compressive strength of concrete was approximately 29.4 N/mm². The dimensions, arrangement of reinforcement are shown in Fig. 8.

The specimens were loaded cyclically by deformation control. Taking the yield deformation as a reference value, the load was increased incrementally with three cycles of application at each stage.

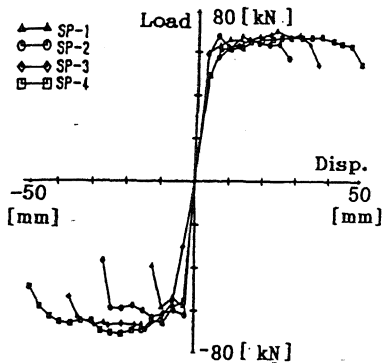


Fig. 9 Load deflection envelope curve

3.1 Load-deflection relationships

Fig. 9 shows the envelope curves of load deflection relationships of four specimens. The steel plate wrapping increased the load carrying capacity a little (No. 3 and, No. 4), compared with the specimen with hoops (No. 2). However, its role was remarkable for prevention against the drastic reduction of capacity at large deflection levels. The combination of hoops and steel plate (No. 4 specimen) presented this characteristics very notable.

The critical deformation for ductility evaluation was taken when the peak capacity at any cycle of load decreased below

the first yield capacity. The ductility ratio μ_d was then calculated as the ratio of the critical deflection to the first yield deflection. The ductility ratios of specimens are shown in Table 2.

Table 2. Ductility ratios

Spec. No.	μ_d
1	4.2
2	8.0
3	12.5
4	13.6

3.2 Estimation of ductility

The basic idea to estimate the ductility of columns was that the deflection after peak load was mainly concerned with the inelastic rotation of the fracture process zone, and that the inelastic was mainly influenced by the stress-strain behavior of confined concrete unless longitudinal tension reinforcement broke out. Taking the influence of sliding out of longitudinal bars into account, the stress-strain curve of bars was idealized as shown in Fig.10.

First, the moment-curvature relationship should be calculated, then, the displacement at the first yield is given as

$$\delta_y = \int_0^a \phi(x) \cdot (1-x) dx \quad (19)$$

where a = distance from the column fixed end to the loading location.

Plastic rotation is assumed occur over the zone of strain localization w of Eq. 16, and concentrated at the center; The total displacement δ_u is given by

$$\delta_u = \delta_y + (\phi_u - \phi_y) \cdot w \cdot (a - 0.5w) \quad (20)$$

where ϕ_y and ϕ_u can be taken from the moment curvature diagram Fig. 12(a).

The displacement ductility is then evaluated as $\mu_d = \delta_u / \delta_y$. The displacement ductility ratios for the four specimens are indicated in Table 3

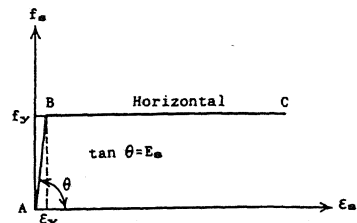


Fig. 10 Idealized steel stress-strain curve

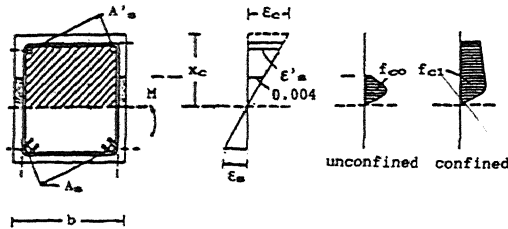
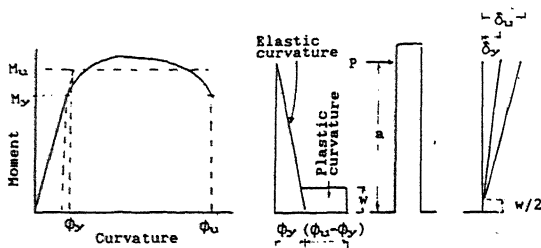


Fig. 11 Conditions for the $M-\phi$ calculation



(a) Moment-curvature relationship (b) Curvature and displacement of member.

Fig. 12 Conditions for the displacement ductility calculation

Table 3. Displacement ductility ratio

Spec. No.	μ_d
1	3.5
2	6.4
3	9.8
4	11.5

4 CONCLUSION

Taking account of strain localization, the effect of confinement by various reinforcement was evaluated quantitatively in terms of size of fracture process zone and the stress-strain characteristics in the zone.

Although the evaluation of ductility of RC columns was not necessarily good enough, the approach discussed in this paper showed the possibility to estimate the ductility of RC members in a common manner.

REFERENCES

Avilés, N. B. and Maruyama, K. 1991. Some considerations on ductility of RC members, International Symposium on Natural Disaster and Civil Engrg., JSCE: 159-165.
 Darwin, D. and Nmai, C.K. 1986. Energy dissipation in RC beams under cyclic load, J. Struct. Engrg., ASCE, Vol. 112,

No. 8: 1829-1846.
 Ehsani, M. R. and Wigth, J. K. 1990. Confinement steel requirements for connections in ductile frames, J. Struct. Engrg., ASCE, Vol. 116, No. 3: 751-767.
 Nakatsuka, T., Suzuki, K., and Inoue, K., (1988). Stress-strain characteristics of confined concrete with circular reinforcement and buckling behavior, Colloquium on Ductility JCI: 21-32 (in Japanese).
 Park, R., Priestley, M. J. N. and Gill, W.D. 1982. Ductility of square confined concrete columns, J. Struct. Div., ASCE, Vol. 108, No. 4: 929-950.
 Samra, R. M. 1990. Ductility analysis of confined columns, J. Struct. Engrg., ASCE, Vol. 116, No. 11: 3148-3161.
 Scott, B. D., Park, R. and Priestly, M. J. N. (1982). Stress-strain behavior of concrete of confined by overlapping hoops at low and high strain rates, J. ACI., Title 79-2: 13-27.
 Shah, S., Fafitis A. and Arnold R. 1983. Cyclic loading of spirally reinforced concrete, J. Struct. Engrg., ASCE, Vol. 109, No. 7: 1695-1711.
 Sheikh, S. A. and Uzemuri, S. M. 1982. Analytical model for concrete confinement in tied columns, J. Struct. Engrg., ASCE, Vol. 108, No. 12: 2703-2722.
 Park, R., Kent, D.C. and Sampson, R. A. 1972. Reinforced concrete members with cycled loading, J. Struct. Div., ASCE, Vol. 98, No. ST7: 1341-1360.
 Russo, G. 1990. Beam strength enhancement at design ductility factors demands, J. Struct. Engrg., ASCE, Vol. 116, No. 12: 3402-3413